



Time-dependent response of the global ocean clathrate reservoir to climatic and anthropogenic forcing

David Archer and Bruce Buffett,

Department of the Geophysical Sciences, University of Chicago, 5734 South Ellis Avenue, Chicago, Illinois 60637, USA (d-archer@uchicago.edu)

[1] Buffett and Archer (2004) showed a model of the steady state global ocean clathrate reservoir that reproduces drill data and predicts a global methane inventory of about 5000 Gton C. The model inventory is very sensitive to ocean temperature, with factor-of-two changes in methane inventory in response to temperature changes of 1.5°C. Here we explore the potential time-dependent behavior of the clathrate reservoir, assuming simple first-order rate constants for methane accumulation and meltdown in response to changes in the predicted steady state reservoir. For melting, we divide the reservoir into two parts, one melting catastrophically and the other slowly. Evolution of clathrates through geologic time is very sensitive to the choice of these rate constants. A positive feedback exists during a transient meltdown event, stronger if the catastrophic-melting fraction is high and its melting timescale is fast. A clathrate reservoir governed by such kinetics would melt down periodically, on a multimillion-year timescale determined by the rate constant for clathrate accumulation. Ideally, we would like a model that predicts runaway melting in the Paleocene and stability in the Pleistocene. However, the model is most unstable when climate is cold, rather than warm. Opting for stability in the Pleistocene constrains the melting kinetic parameters, leaving one degree of freedom. The grow-in timescale must be 5 Myr or longer, to get the deglacial $\delta^{13}\text{C}$ right, but shorter than 10 Myr, in order for clathrates to have built up through geologically recent cooling. The model thus constrained predicts methane fluxes of 200 Gton C or less on deglaciations, but eventual releases of 2000–4000 Gton C in response to a ~ 2000 Gton C anthropogenic carbon release. Anthropogenic climate change differs from a deglaciation in that it warms the ocean to temperatures not seen in millions of years.

Components: 6871 words, 12 figures.

Keywords: methane; clathrate; hydrate; climate; ocean.

Index Terms: 0428 Biogeosciences: Carbon cycling (4806); 0414 Biogeosciences: Biogeochemical cycles, processes, and modeling (0412, 0793, 1615, 4805, 4912); 0714 Cryosphere: Clathrate; 1009 Geochemistry: Geochemical modeling (3610, 8410); 1051 Geochemistry: Sedimentary geochemistry.

Received 1 October 2004; **Revised** 18 November 2004; **Accepted** 12 December 2004; **Published** 3 March 2005.

Archer, D., and B. Buffett (2005), Time-dependent response of the global ocean clathrate reservoir to climatic and anthropogenic forcing, *Geochem. Geophys. Geosyst.*, 6, Q03002, doi:10.1029/2004GC000854.

1. Introduction

[2] Under cold, high pressure conditions, water and methane freeze into a crystalline structure called clathrate or hydrate [Buffett, 2000]. Most of the clathrates on earth are located in methane-filled sediments along coastal margins. In most

locations, the isotopic signature of the carbon in the methane indicates a biological source that is fed by sedimentary organic matter. The total inventory of clathrate-bound methane is estimated to be comparable to the inventory of fossil fuel carbon, order 3000–15000 Gton C [Buffett and Archer, 2004; Kvenvolden, 1993; MacDonald, 1990b].

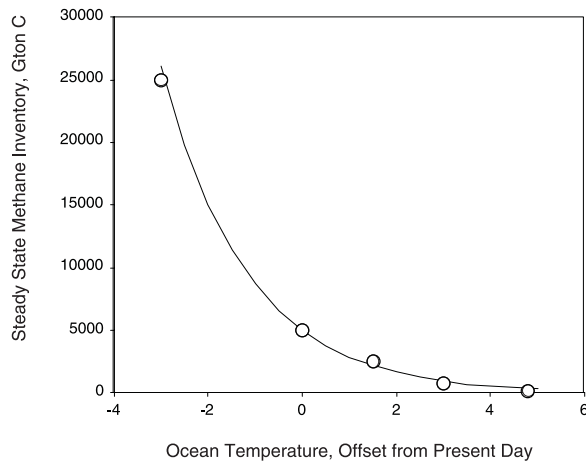


Figure 1. Steady state inventory of methane in the clathrate reservoir, as a function of ocean temperature, offset from present-day (modified from *Buffett and Archer* [2004]).

[3] Clathrate accumulation is limited by the supply rate of organic matter to the seafloor and its subsequent biological processing into methane. Time-dependent models of the sediment column indicate that it may take several million years to build up methane to the steady state column inventory [*Davie and Buffett*, 2001]. In contrast, data from the geochemical record, and from pockmarks and landslide deposits on the seafloor [*Hovland and Judd*, 1988], suggest that the timescale for a collapse might be much faster. The timescale of the purported clathrate collapse during the Paleocene Eocene Thermal Maximum, in particular, was about 10 kyr [*Dickens*, 2001a].

[4] In this paper we consider the behavior of the global ocean clathrate reservoir on geologic timescales, in the past and in the future. *Buffett and Archer* [2004] constructed a model of the steady state global ocean clathrate reservoir. Here we explore the potential time-dependent behavior of the clathrate reservoir, assuming simple first-order rate constants for methane accumulation and melt-down approach to the steady state inventory as a function of ocean temperature. For melting, we assumed two reservoirs, one melting catastrophically (releasing carbon on a timescale of 1 kyr or longer) and the other slowly (millions of years governed by the molecular diffusion timescale). We use this kinetic formulation to explore the time evolution of the clathrate reservoir through the cooling since the middle Miocene, and the potential for glacial/interglacial and global warming response of the clathrate reservoir.

[5] Several studies have considered the response of marine clathrates to climate change in the coming century, and concluded that it would be small [*Gornitz and Fung*, 1994; *Harvey and Huang*, 1995]. To a large extent this is because it takes roughly a millennium to change the temperature of the deep ocean [*Stouffer and Manabe*, 2003], and perhaps another for any thermal perturbation to reach the depth of the hydrate deposits in the sediment column. On time frames of thousands of years, we predict the clathrate inventory to be quite sensitive to anthropogenic carbon forcing.

2. Model Description

[6] The Buffett and Archer steady state clathrate inventory model is based on (1) a parameterization of the ocean carbon cycle which delivers organic carbon to the seafloor, (2) a sediment diagenesis model which predicts the efficiency of organic carbon preservation to the methanogenesis zone as a function of carbon rain and overlying water oxygen [*Archer et al.*, 2002], and (3) a methane clathrate geophysical model [*Davie and Buffett*, 2003] which predicts the steady state inventory of dissolved, frozen, and gaseous methane per square meter of seafloor.

[7] For the present-day mean ocean temperature profile, the model predicts a methane inventory of 3000 Gton C in clathrate. Another 2000 Gton C is trapped as methane bubbles in the underlying sediments. The predictions are sensitive to fluid flow; in the extreme case of no flow we arrive at a combine clathrate and bubble inventory of 1250 Gton C. The model is also sensitive to the efficiency of organic carbon conversion to methane; the model requires a value of 25% conversion in order to match ODP chlorinity and sulfate data. The present-day model inventory estimate is on the lower end of conventional estimates [*Kvenvolden*, 1988; *MacDonald*, 1990a], because the average clathrate and bubble volumes predicted by the model are lower than previously assumed. On the other hand, our predicted inventory is higher than a recent estimate of *Milkov* [2004], which is based on new observations from ODP Leg 204, off the coast of Oregon. The shallow water depth at Leg 204 yields unusually low clathrate volumes in the model (and the observations), suggesting that this site may not be representative of the entire clathrate inventory.

[8] The model steady state methane inventory is extremely sensitive to ocean temperature (Figure 1). A temperature increase of 3°C, such as would persist

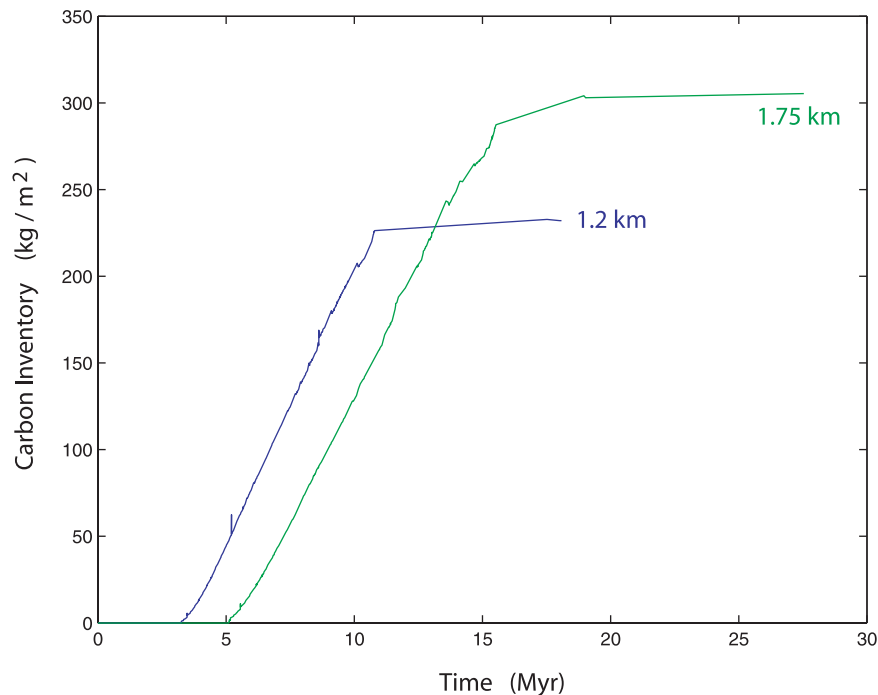


Figure 2. Time-dependent predictions of the clathrate model [Davie and Buffett, 2001], showing the buildup of the column inventory of clathrate at two representative water depths. The buildup is initiated by lowering the seafloor temperature by 3°C. Clathrate is initially absent from the sediments, and the starting concentration of dissolved methane is given by the steady state solution at the initial temperature.

10 kyr after a 5000 Gton carbon release, drives the steady state methane inventory down to 800 Gton C. The oxygen concentrations are taken as unchanged in this calculation, in spite of the decreasing solubility of O₂ with increasing temperature, for simplicity and because it would take millions of years for an oxygen-driven increase in organic carbon burial to fuel an increase in methane production. Temperature-driven oxygen changes are thus irrelevant on the fast timescale of a melting event. On timescales of millions of years, the oxygen concentration of the ocean is probably regulated by the burial of organic matter [Cappellen and Ingall, 1996], and not simply determined by temperature.

[9] The model temperature sensitivity can be decomposed into two components. One component is due to the decrease in the global volume of the stability zone; our estimate is comparable to that obtained in a previous study [Dickens, 2001b]. The other component is due to an increase in the concentration of sedimentary organic matter required to saturate the pore water with methane. As a rule of thumb, clathrate is found today in sediments where organic carbon exceeds 1% dry weight. If the temperature were increased by 3°C, the model predicts that ~2.5% organic carbon would be required, decreasing the area of clathrate

formation dramatically [Buffett and Archer, 2004]. The only way we have found to decrease the temperature sensitivity of the clathrate reservoir is to decrease the present-day estimate of the clathrate inventory, which is already lower than many generally accepted estimates.

[10] The Buffett and Archer model explicitly determines the steady state inventory of methane in the sediment column, where sources and sinks balance perfectly. Here we use these results to construct a time-dependent evolution of the clathrate reservoir in the past and future. A true mechanistic model of global clathrate buildup is technically feasible [Davie and Buffett, 2001], but the mechanisms by which the clathrate reservoir decreases in size are poorly constrained, with the possibilities ranging wildly from catastrophic meltdown to gradual diffusive and chemical loss of methane with no release of carbon to the atmosphere and ocean at all. We take the approach of parameterizing the growth and decay of the clathrate inventory using simple first-order relaxation toward the steady state value.

[11] The timescale of clathrate buildup is slow, limited by the supply rate of bacterial methanogenesis from breakdown of organic matter. The rate and carbon-conversion efficiency of methanogene-

sis are difficult to measure directly, but these are tunable parameters in the steady state model, to which the steady state inventory is sensitive. Values for these parameters are chosen to reproduce available observations for clathrate volumes and pore water composition. The same set of internally consistent parameters are used in the time-dependent model of the *Davie and Buffett* [2001] to assess the rate of clathrate accumulation in response to cooling. The response time depends on whether clathrate is initially present in the sediments, because it takes time to build up the dissolved methane concentration to saturation levels. A steady state can be established within a few Myr when clathrate is initially present in the sediment. However, most of the increase in the steady state inventory occurs in regions where clathrate is not present prior to cooling. Time-dependent calculations with an initially undersaturated concentration of dissolved methane and no clathrate adjust to an equilibrium state within 5–10 Myr (Figure 2).

[12] The mechanisms by which the clathrate reservoir might decrease in size are more varied, and more difficult to constrain. Pockmarks and landslide deposits on the seafloor document occasional catastrophic releases [*Hovland and Judd*, 1988; *Maslin et al.*, 1998, 2004], which may be triggered by earthquakes, sediment loading, or isostatic rebound. The catastrophic interaction with temperature scenario would be for clathrate to melt at the base of the stability zone, generating bubbles of methane [*Kayen and Lee*, 1991]. The increase in volume accompanying this transition increases the hydrostatic pressure of the sediment column, destabilizing the sediment pile to landslides. Eventually, the excess hydrostatic pressure spike diffuses away, so this mechanism might be more responsive to faster temperature perturbations. The methane release from a single landslide would be fast, but the decomposition of the entire clathrate reservoir would probably be accomplished by a series of landslides, rather than a single catastrophic event. Clathrate deposits in the Arctic Ocean may respond first to global warming, because they are found at shallow depths in the cold water column, and because warming is most intense in high latitudes. Our model will not resolve special cases like these in this paper. The minimum response time of the global clathrate reservoir overall to thermal forcing is determined by sediment column warming time-scale, several thousand years.

[13] Another mechanism would involve the coalescence of methane bubbles into channels that

seep through the sediment of their own accord [*Flemings et al.*, 2003]. The extent to which this occurs probably depends on the volume fraction of the initial hydrate, so that only a fraction of the unstable methane would be released by this mechanism. The timescale for this process would be slowed somewhat by diffusion of dissolved methane from smaller to larger bubbles.

[14] A third possible response is for the released methane to diffuse away, reacting with sulfate to generate sedimentary CaCO_3 . The timescale for molecular diffusion from the stability zone to the seafloor is long, millions of years. Even if some of the clathrate carbon reached the ocean as CO_2 , the silicate weathering thermostat buffers atmospheric pCO_2 on timescales of ~ 400 kyr [*Berner and Caldeira*, 1997], and would mitigate the climate impact of any clathrate carbon release that was slower than that.

[15] Our kinetic model for the clathrate reservoir is based on a single time constant for methane buildup, $\tau_{\text{grow-in}}$, which we will assume to be of order 5–10 Myr. Clathrate melting is more complicated, but can be approximated by dividing the reservoir into two components, one responding catastrophically to a warming on a timescale denoted τ_{fast} , and another responding slowly, governed by a timescale τ_{slow} set by molecular diffusion. The fraction of the reservoir that melts quickly we will denote as F . We will explore the behavior of the clathrate reservoir within the climate system, as a function of these uncertain parameters.

3. Model Behavior and Sensitivity

[16] Given some fraction of the clathrate reservoir that responds quickly to warming, we find an amplifying feedback, as released carbon amplifies the initial warming perturbation.

[17] Methane itself is a powerful greenhouse gas, and the climate impact of a large methane release to the atmosphere could be intense. However much of the methane may be oxidized to CO_2 within the ocean rather than reaching the atmosphere, depending on the mechanism of clathrate release. In any case, the lifetime of methane in the atmosphere is short relative to the thermal inertia of the deep ocean. We therefore neglect the direct radiative impact of methane in our clathrate stability analysis, and consider only the role of the resulting CO_2 .

[18] CO_2 , the oxidation product of methane, is also a greenhouse gas. The amount of CO_2 that is

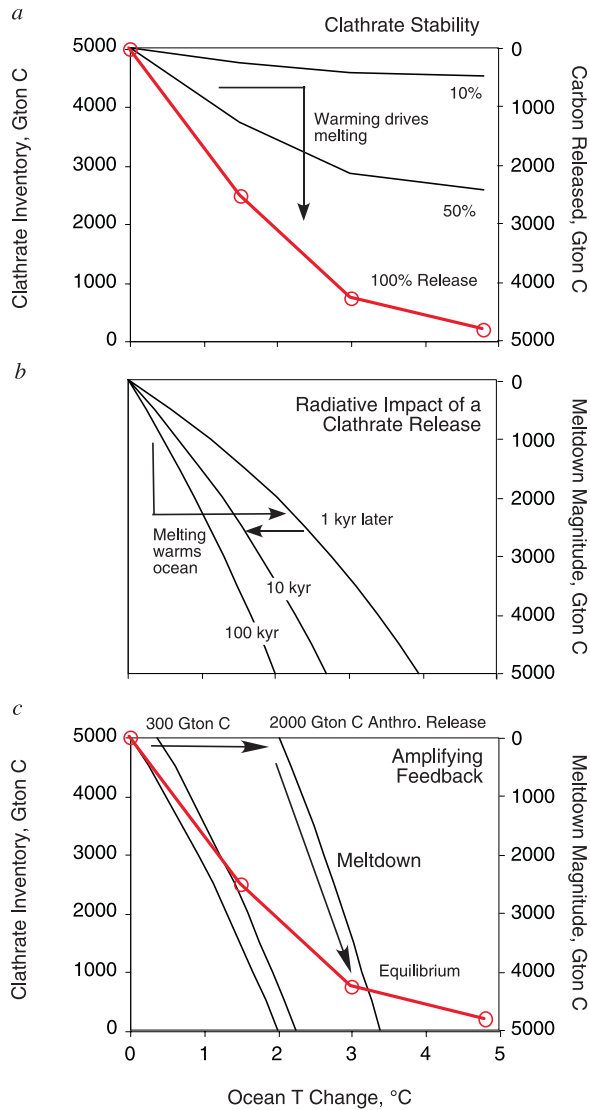


Figure 3. Interaction between ocean temperature and clathrate inventory. (a) Carbon release from clathrates as a function of an ocean warming, assuming 100%, 50%, and 10% carbon release fractions. (b) Ocean temperature as a function of a clathrate meltdown. As the CaCO_3 and silicate weathering cycles restore atmospheric CO_2 toward an equilibrium value (Figure 1), the temperature perturbation also decays with time. (c) Positive feedback between ocean temperature and clathrate melting. An initial anthropogenic carbon release drives clathrates to melt, amplifying the warming. The strength of the amplifier depends on the relative slopes of the stability and radiative impact curves.

vulnerable to melting event is determined by the extent of disequilibrium due to the temperature change and the fast-melting fraction F (Figure 3a). Once released to the atmosphere or ocean, CO_2

equilibrates between these two phases on a timescale of about 300 years, finding an equilibrium where initially 15–30% of the released C resides in the atmosphere, depending on the magnitude of the C release, ranging from 300 to 5000 Gton C (D. Archer, Long-term atmospheric lifetime of fossil-fuel CO_2 , submitted to *Journal of Geophysical Research*, 2004). The carbonate and silicate weathering cycles then act to neutralize the remaining C, removing it from the atmosphere on timescales of thousands to hundreds of thousands of years.

[19] Climate model results and paleoclimate studies suggest that the temperature sensitivity of the deep sea roughly parallels that of the mean earth surface. A coupled ocean/atmosphere model run to equilibrium under a range of $p\text{CO}_2$ values predicts a deep sea warming “climate sensitivity” ΔT_{2x} of 3°C per doubling CO_2 [Stouffer and Manabe, 2003]. The deep ocean temperature during the last glacial maximum was $3\text{--}4^\circ\text{C}$ colder than today [Adkins et al., 2002; Martin et al., 2002], and $8\text{--}12^\circ\text{C}$ warmer than present-day during the Cretaceous and Eocene warm climates [Zachos et al., 2001] (Figure 4). The model results are if anything conservative relative to the paleodata, which are affected by factors other than CO_2 , such as ice albedo forcing during glacial time or changes in atmospheric methane or continental configuration in the deeper past. We rely therefore on the model-derived deep sea temperature sensitivity ΔT_{2x} of 3°C per doubling CO_2 . The radiative forcing due to a carbon release (Figure 3b) is most extreme after just 1000 years, after the ocean temperature has had a chance to respond but before the CO_2 is neutralized by CaCO_3 and silicate rock weathering. With CO_2 neutralization, the thermal perturbation vanishes, ultimately on the silicate thermostat timescale of 400 kyr [Berner and Caldeira, 1997].

[20] The simultaneous back-and-forth relationships between clathrate stability as a function of ocean temperature, and the temperature change as a function of clathrate carbon release, combine to create a positive feedback during a melting event. An initial increase in temperature, resulting from anthropogenic carbon release, increases the temperature of the ocean with no initial change in the clathrate reservoir (Figure 3c). The ocean clathrate reservoir melts down to a new equilibrium, following the radiative impact trajectory (black line). If the carbon perturbation is small, we can predict the intensity of the feedback using a linear stability analysis. The relative slopes of the clathrate inven-

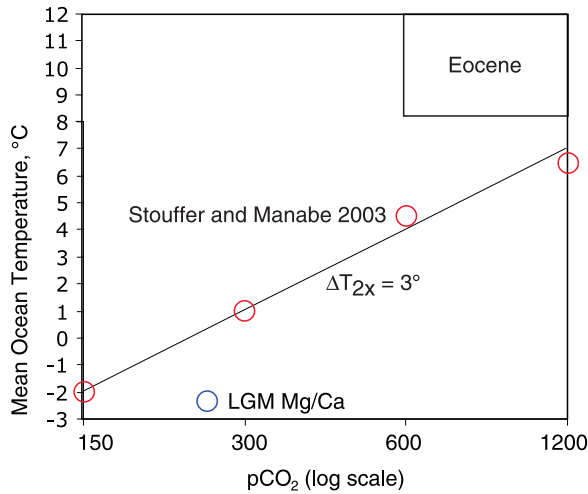


Figure 4. Deep ocean temperature as a function of atmospheric $p\text{CO}_2$, model, and paleoclimate results. Red circles are equilibrium atmospheric/ocean climate model results [from *Stouffer and Manabe, 2003*]. LGM cooling (blue circle) is based on Mg/Ca data in benthic foraminifera [*Martin et al., 2002*] and deep pore water results [*Schrag et al., 1996*]. This cooling is due in part to ice sheet albedo forcing and is therefore an overestimate of the sensitivity to CO_2 alone. Eocene temperatures are based on $\delta^{18}\text{O}$ and Mg/Ca [*Archer et al., 2004*], and $p\text{CO}_2$ is consistent with paleosol $\delta^{13}\text{C}$ and geochemical model [*Berner, 1997*] results.

tory and radiative relationships determine the magnitude of the feedback, as shown in Figure 3c. Defining α_S as the slope of the clathrate inventory expressed in units of $\text{Gton C}/^\circ\text{C}$, and α_R as the slope of the radiative impact of a clathrate release in the same units, the strength of the feedback can then be calculated as

$$A = \alpha_S / (\alpha_R - \alpha_S),$$

where A is defined as

$$\Delta p\text{CO}_2(\text{full}) = \Delta p\text{CO}_2(\text{anthro}) \cdot (1 + A).$$

[21] The value of the temperature response to a carbon release of a given magnitude, α_R , depends on the timescale over which the clathrate inventory responds. A carbon release generates a 1 kyr spike of temperature in the deep sea, which then decreases with time as carbon is assimilated into the CaCO_3 cycle in the ocean and the silicate weathering geochemical cycle. If the fast-melting response time, τ_{fast} , is 10 kyr, the clathrate reservoir can withstand a 1 kyr thermal spike, and the appropriate temperature sensitivity to a carbon release, α_R , can be approximated as the tempera-

ture of the ocean 10 kyr after the carbon release. The atmospheric fraction of a small (300 Gton C) carbon release to an ocean circulation/sediment carbon cycle model [*Archer and Maier-Reimer, 1994*] is shown as a function of time in Figure 5a. The value of α_R calculated using the atmospheric fraction is shown in Figure 5b. The dependence of α_R on timescale can also be envisioned by noting the different slopes of the radiative response curves in Figure 3b. The amount of carbon released by a temperature perturbation of a given magnitude, α_S , depends simply on the release fraction F (Figure 5c; see also Figure 3a).

[22] The stability analysis predicts that the amplifier strength, A , depends very strongly on τ_{fast} and F (Figure 6). If only 10% of the excess methane escapes from the sediments, and the timescale for this response is 100 kyr, then the amplifying feedback is weak ($A \sim 0.1$). If half of the reservoir responds in 1 kyr, the analysis predicts that clathrate deposits in the ocean would be unconditionally unstable. A τ_{fast} of 10 kyr, derived from the PETM record, is also unstable, unless the release fraction $F < 0.6$. If half of the reservoir responds on a timescale of 10 kyr, then the amplifier A has a magnitude of 2.4. The slopes α_R and α_S , and hence the amplifier A , change with the size of the clathrate inventory. A large inventory is inherently more unstable than a small inventory, so a stable reservoir at warm temperatures could become unstable with cooling.

[23] For a significant range of τ_{fast} and F , the reservoir melts down with no anthropogenic forcing at all (labeled “Unstable Region” in Figure 6). If the real clathrate reservoir were this unstable, the clathrate reservoir would melt down periodically whenever the clathrate inventory gets too large, as diagrammed in Figure 7. Beginning the cycle with a low clathrate inventory, methane would accumulate, on a timescale of millions of years, approaching equilibrium. This part of the cycle is labeled “a” in Figure 7. The equilibrium value itself is unstable, and the clathrate reservoir becomes increasingly sensitive to small ocean temperature perturbations as equilibrium is approached. Following such a temperature perturbation, (labeled “b”) the clathrate reservoir melts down, warming the deep sea as it does, until a new equilibrium is reached with a lower clathrate inventory (trajectory “c”). The temperature spike generated by the meltdown lasts for ~ 400 kyr, after which time the CO_2 is assimilated into the silicate weathering cycle (trajectory “d” in Figure 7). The result is a

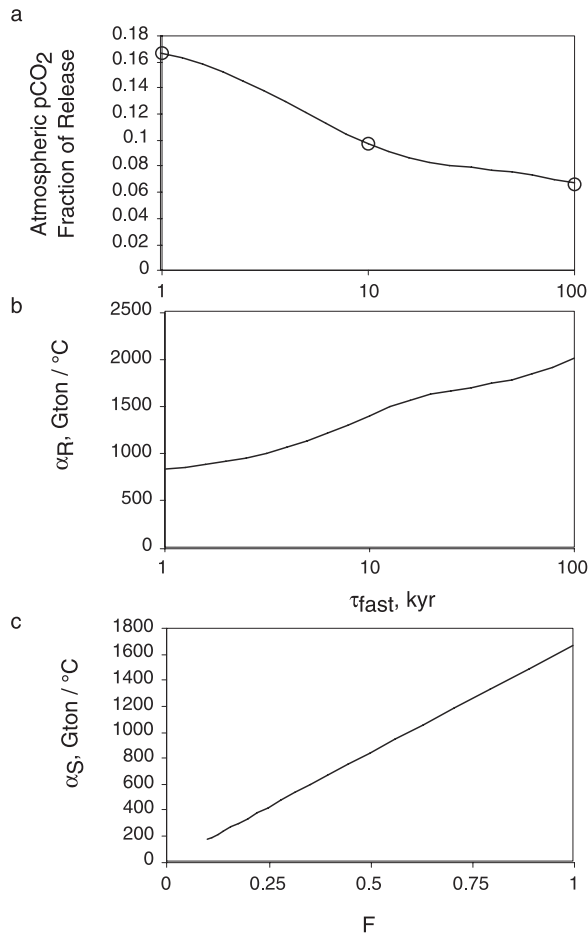


Figure 5. (a) Atmospheric fraction of a 300 Gton C carbon release as a function of time from the release. pCO₂ decreases with time as the pH of the ocean is restored by the CaCO₃ cycle. (b) The value of α_R , the deep ocean temperature response to a small carbon release of a given magnitude, depends only on the amount of time elapsed since the carbon release. If the response time of the clathrate inventory is 10 kyr, for example, then the atmospheric pCO₂ 10 kyr from the carbon release is the appropriate radiative sensitivity to calculate the feedback amplification, A (see text). (c) The sensitivity of the clathrate release to temperature depends solely on the release fraction, F.

periodic meltdown of most of the clathrate reservoir, occurring on a timescale set by methane accumulation: millions of years.

[24] These periodic meltdowns would get more intense with cooling climate, since a cold ocean permits more clathrate than a warm ocean. The slope α_S increases such that the amplification factor from the temperature feedback during melting events becomes more intense, i.e., toward instability. Carbon isotope excursions are common

in the geologic record, which might be explained as runaway meltdown events. However, there is nothing like this from the Pleistocene, when the earth is coldest and the record the cleanest. It seems reasonable to assume that the parameters for clathrate melting should not predict unstable behavior in present-day conditions.

[25] The time dependence of the clathrate reservoir exerts primary control over the inventory of methane, because the time constant for buildup is long relative to the timescale of thermal forcing over recent earth history. We subjected the model to a steady ramp of decreasing temperature since the Mid-Miocene Optimum 15 Mya, followed by glacial/interglacial ocean temperature cycles and one super-interglacial crudely representative of the Anthropocene (Figure 8). Because model temperature is imposed, this model does not include the temperature feedback mechanism described above. Therefore it is only applicable to the stable region of parameter space. The clathrate inventory relaxes toward the equilibrium value using the kinetic formulation described above. The value of $\tau_{grow-in}$ is comparable to the timescale for long-term climate evolution. Using $\tau_{grow-in}$ of 10 Myr, we find that the reservoir would just now be approaching equilibrium with the warm spikes of the interglacial periods (red curve). If the reservoir

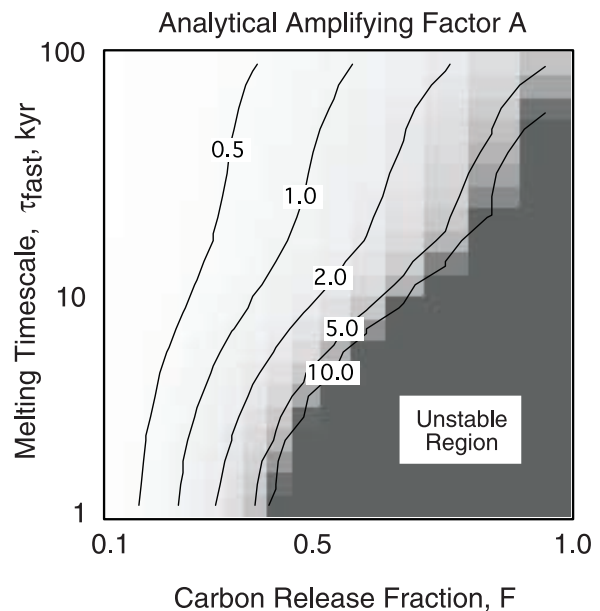


Figure 6. Analytical calculation of the amplifier strength as a function of clathrate equilibration timescale τ and carbon release fraction F. If τ were fast and F large, the clathrate inventory would be unstable and might not exist today.

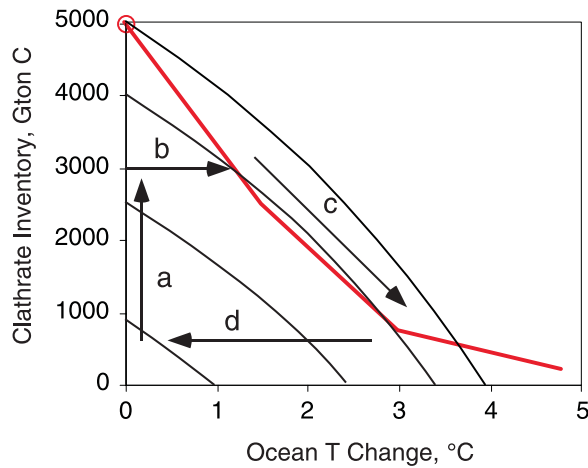


Figure 7. Dynamical schematic of a clathrate reservoir accumulate-purge cycle that would result if the meltdown response timescale is fast (1 kyr) and the carbon release fraction high (100%). (a) The grow-in phase would take millions of years, paced by the delivery rate of organic carbon to the methanogenesis zone (ref). (b) As the clathrate inventory approaches equilibrium (the red line), a small thermal perturbation could drive the clathrate inventory to exceed equilibrium. (c) Following this, the clathrate reservoir would melt down, warming the deep ocean according to the radiative trajectory (black line). (d) The thermal perturbation generated by the carbon release subsides on a timescale of ~ 400 kyr, as the silicate weathering cycle absorbs the excess atmospheric CO_2 .

grows with $\tau_{\text{grow-in}}$ of 5 Myr (blue curve), the reservoir exceeds the interglacial steady state value, and some glacial/interglacial fluxes of methane result. If $\tau_{\text{grow-in}}$ is much longer than 20 Myr, the present-day ocean would be farther from steady state than it apparently is (orange curve) [Buffett and Archer, 2004].

[26] The last 500 kyr are shown in more detail in Figure 9. We have omitted from this figure the $\tau_{\text{grow-in}} = 20$ Myr run (orange) and added a fourth (green) run, using $\tau_{\text{grow-in}}$ of 5 Myr and τ_{fast} of 20 kyr (as opposed to 10 kyr for the red and blue curves). Both of the 5 Myr grow-in models exhibit glacial/interglacial fluxes of methane. Both release about 175 Gton C during deglaciations, in spite of the differences in τ_{fast} . Interestingly, we find that after the model has reached a glacial cycle quasi-steady state, the magnitude of the deglacial methane release is determined by how fast the reservoir grows ($\tau_{\text{grow-in}}$), rather than how fast it melts (τ_{fast}). The relationship between $\tau_{\text{grow-in}}$ and the deglacial methane release is shown in Figure 10. These deglacial carbon fluxes are comparable to variations in the terrestrial biosphere [Crowley, 1995;

Shackleton, 1977]. The isotopic signatures of methane and terrestrial organic matter are combined with the isotopic composition of the ocean and atmosphere to yield the $\delta^{13}\text{C}$ isotopic record. A large methane release would require a larger terrestrial carbon uptake to account for the $\delta^{13}\text{C}$ [Maslin and Thomas, 2003]. With no methane release, we require terrestrial carbon uptake of approximately 500 Gton C [Shackleton, 1977]. This is somewhat lower than terrestrial ecosystem models tend to suggest [Crowley, 1995]. However, as we increase the methane and terrestrial carbon fluxes, we have a more difficult time explaining the glacial/interglacial atmospheric pCO_2 cycles, as the net (methane + terrestrial) carbon uptake on deglaciation must be overcome by whatever mechanism drives atmospheric pCO_2 in the opposite direction, toward higher values during the interglacial [Archer et al., 2000]. In spite of these uncertainties, the recent

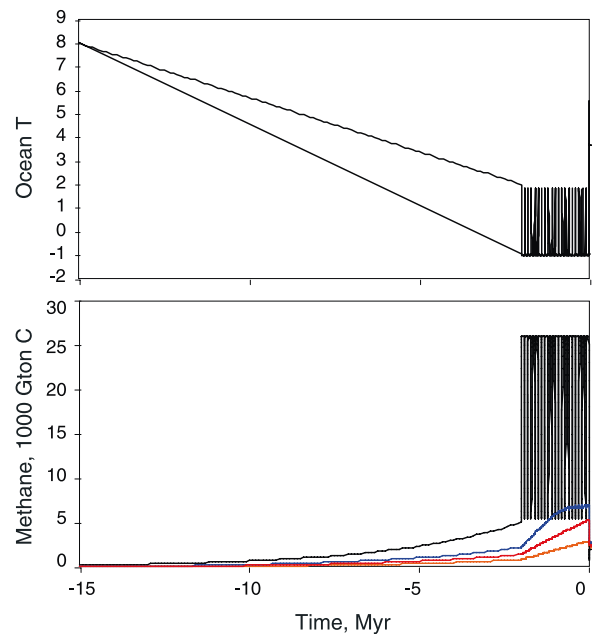


Figure 8. Potential time evolution of the methane clathrate inventory through geologic time since the Miocene Climatic Optimum 15 Myr ago. (a) We idealize the temperature history as a linear cooling from an initial temperature of 8°C down to 2°C at the beginning of the Pleistocene. Glacial/interglacial cycles follow every 100 kyr for 2 Myr at the end of the time series. For an expansion of the last few glacial cycles, see Figure 9. (b) Methane inventory results. The black line is the potential, steady state inventory, obtained from the relation shown in Figure 1. Orange, red, and blue lines are time-dependent model results, using grow-in timescales of 20, 10, and 5 Myr, respectively. Both assume 10 kyr and 10 Myr fast and slow meltdown timescales, respectively, with 50% of the inventory attributed to each.

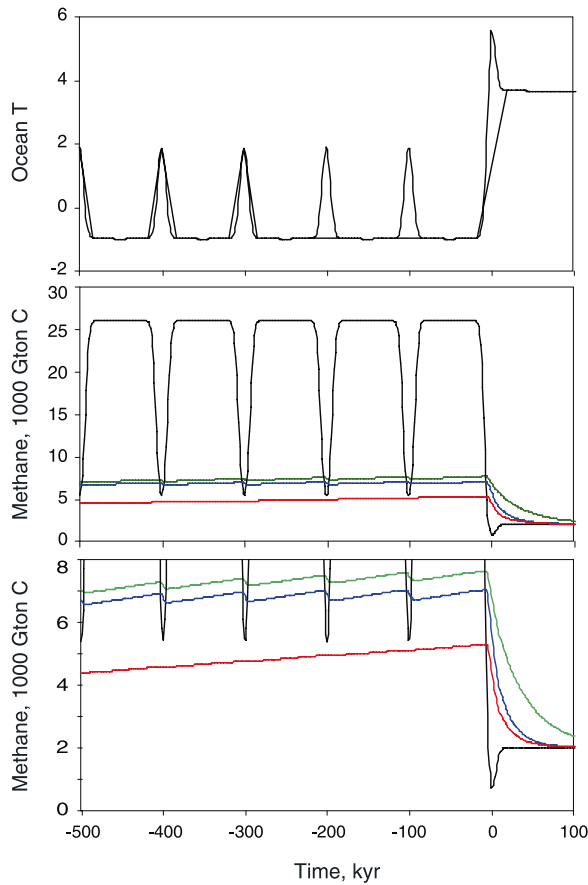


Figure 9. Results from the end of the simulation in Figure 8, expanded to show glacial/interglacial detail. (a) Ocean temperature. The glacial cycles are followed by a “super interglacial” representing the Anthropocene. (b and c) Red and blue curves are as defined in the Figure 8 caption, and the green curve is as the blue but with a fast-melting timescale of 1 kyr. The superwarming of the Anthropocene, because it takes the ocean into temperatures warmer than had been seen in millions of years, predicts a substantially larger clathrate release of 2000–4000 Gton C. Figures 9b and 9c differ only in their vertical scale.

$\delta^{13}\text{C}$ record seems to argue for a build-up timescale $\tau_{\text{grow-in}}$ of 5 Myr or longer.

[27] Reasonable values for the grow-in timescale, $\tau_{\text{grow-in}}$, would seem to be in the range of 5–10 Myr. If it were longer, the clathrate reservoir would be too far from steady state; if it were shorter, there is too much methane released on deglaciations. From the stability analysis, we have coupled ranges of τ_{fast} and the fast-melting fraction, F . For values of τ_{fast} equal to 1, 10, and 100 kyr, the maximum values of F are 0.3, 0.5, and 1.0, respectively. These conditions are marginally stable and thus offer some hope of explaining past $\delta^{13}\text{C}$ anomalies such as the PETM,

without violating the apparent stability of the clathrate reservoir throughout the Pleistocene.

4. Clathrate Reservoir Sensitivity to Anthropogenic Forcing

[28] The response of the clathrate reservoir to anthropogenic carbon release depends on the interplay between clathrate meltdown dynamics and the natural neutralization of released CO_2 , either anthropogenic or from clathrates, by the CaCO_3 and SiO_2 weathering cycles. We explore the interaction between these two dynamics by adding a simple clathrate reservoir to a time-dependent ocean carbon cycle model [Archer and Maier-Reimer, 1994]. The model is based on an off-line ocean tracer advection code called Hamocc2. Biological and chemical fluxes impact the resulting distributions of dissolved carbon and nutrients. A sediment diagenesis model is coupled to each grid point at the seafloor, predicting burial or redissolution of CaCO_3 . The model ocean pH is regulated as is the real ocean by the throughput of CaCO_3 [Broecker and Peng, 1987]. The model flow field is read from a file at the outset of the run and is unaffected by changes in atmospheric pCO_2 . Ocean temperature changes are imposed uniformly through the ocean, affecting only gas equilibrium and gas exchange kinetics calculations. The ocean temperature relaxes toward an equilibrium value

$$\Delta T_{\text{equil}} = 3^\circ\text{C} / \ln(2) \cdot \ln(\text{pCO}_2 / 278)$$

on a timescale of 1 kyr such that

$$\delta T / \delta t = (T_{\text{equil}} - T) / 1 \text{ kyr}.$$

The initial clathrate inventory is taken to be 5000 Gton C. The steady state clathrate reservoir, $\text{Cl}_{\text{steady}}$, is approximated by

$$\text{Cl}_{\text{steady}} = 5000 \text{ Gton C} \cdot e^{(-0.55 \Delta T(^{\circ}\text{C}))}.$$

The fast-melting portion of the clathrate reservoir at any time in the simulation is given by

$$\text{Cl}_{\text{fast}} = \text{Cl} - (1 - F) * 5000 \text{ Gton C},$$

where Cl is the total current inventory. The equilibrium fast fraction is defined as

$$\text{Cl}_{\text{fast,eq}} = F \cdot \text{Cl}_{\text{steady}}.$$

During melting, the clathrate inventory then evolves according to

$$d\text{Cl}/dt = (\text{Cl}_{\text{fast}} - \text{Cl}_{\text{fast,eq}}) / \tau_{\text{fast}}.$$

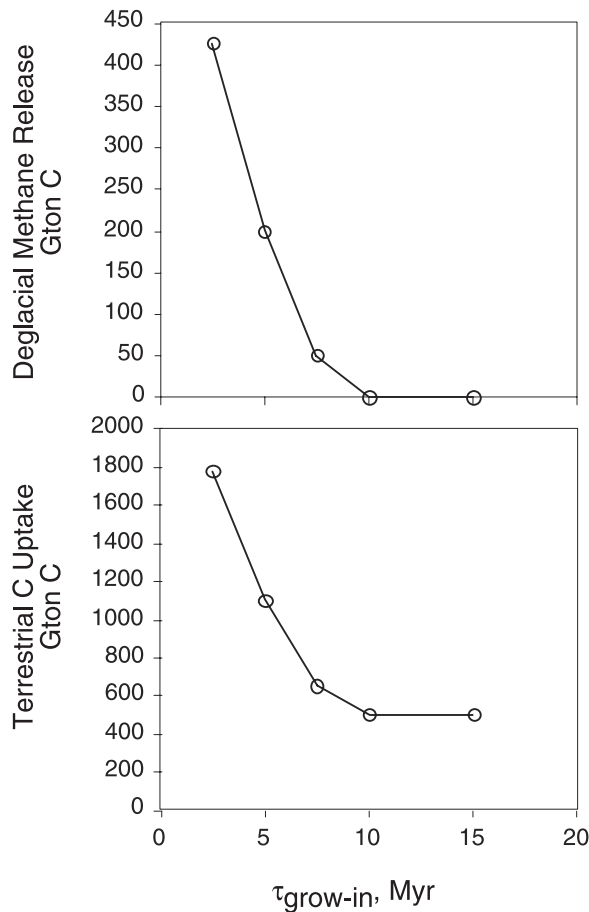


Figure 10. The amount of methane released by ocean clathrates in the model of Figures 8 and 9 depends on the timescale for clathrate accumulation, because the model reaches a quasi-steady state through a glacial cycle where release during warm intervals is balanced by accumulation during cold intervals. (a) The effect of the grow-in timescale on the amount of methane carbon released upon deglaciations. (b) The amount of deglacial carbon uptake by the terrestrial biosphere that is required to accommodate the isotopically light methane release in (Figure 10a) and reproduce the $\delta^{13}\text{C}$ record in the deep sea.

[29] The models were run using a range in τ_{fast} and F values, and the eventual extent of clathrate meltdown, in units of 1000 Gton C, is contoured as a function of those parameters in Figure 11. The results mirror the sensitivity analysis (Figure 6) in that fast τ_{fast} and high F tend to produce a large release of carbon from clathrate and a large amplifying factor.

[30] Assuming that the values of τ_{fast} and F are such that the present-day clathrate inventory is at least marginally stable, we can limit the maximum values of F to 0.3, 0.5 and 1.0, for values of τ equal

to 1, 10, and 100 kyr, respectively. These combinations of parameter values are indicated by solid circles in Figure 11. Results from the time-dependent model, using these values, are shown in Figure 12. In all cases, the long-term pCO_2 increase in the atmosphere is about doubled by the release of clathrate carbon (Figure 12a). The clathrate inventory is projected to lose 1000–3000 Gton C, depending on the amount of anthropogenic carbon released, and the meltdown kinetics of the clathrate reservoir (Figure 12b).

[31] We estimated the atmospheric methane perturbation due to clathrate melting by assuming a 15-year atmospheric residence time of methane

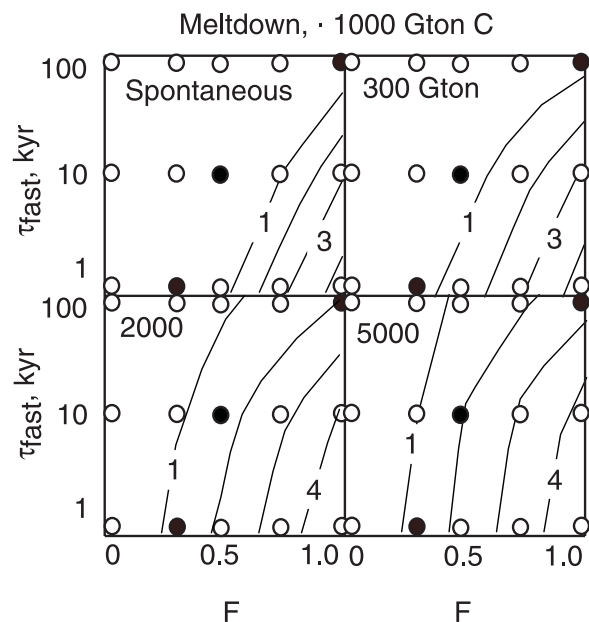


Figure 11. Model simulation of clathrate response to anthropogenic CO_2 release. The ocean carbon cycle and atmosphere/ocean CO_2 equilibrium are determined using an off-line ocean tracer advection and sediment geochemistry code used by Archer and Maier-Reimer [1994]. CaCO_3 burial balances weathering in the initial steady state, and the pH of the ocean is buffered by perturbation of CaCO_3 burial. A silicate weathering feedback [Berner and Kothavala, 2001] restores atmospheric pCO_2 toward 280 ppm on a timescale of 400 kyr. The extent of clathrate melting by the end of the simulation depends on three quantities: the size of an initial anthropogenic CO_2 release (from 0, labeled “spontaneous”), 300, 2000, and 5000 Gton C; the fast-melting timescale τ_{fast} ; and the fast-melting fraction F. Each circle represents one model run. Contours show the extent of clathrate melting after 100 kyr. The solid circles are marginally stable when unprovoked by an anthropogenic carbon release, and so these represent worst-case possibilities for the real world. Solid circle runs are shown in Figure 12.

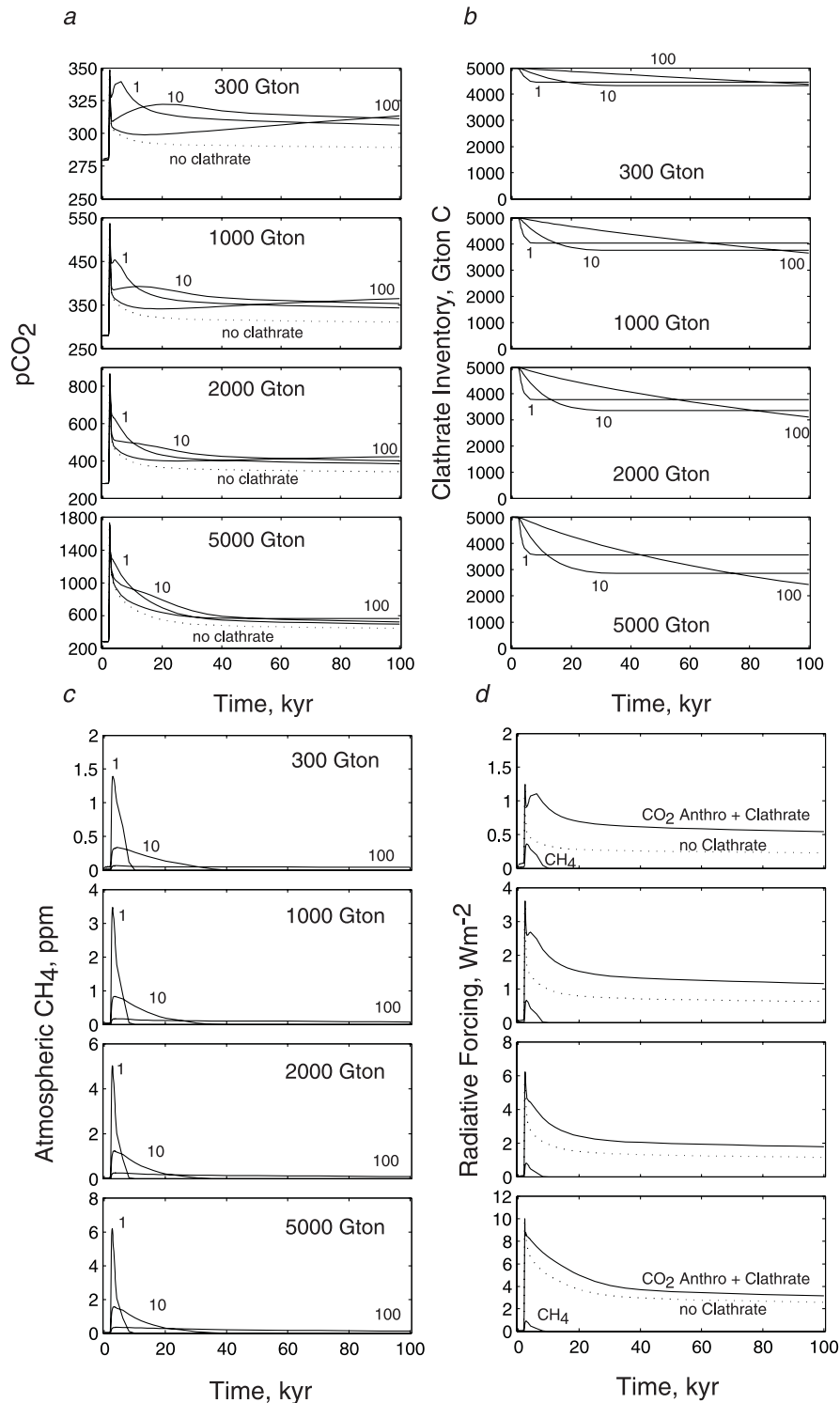


Figure 12. Model simulation of clathrate response to anthropogenic CO₂ release; runs denoted by solid circles in Figure 11. (a) Atmospheric pCO₂, for model runs with no clathrates (dotted lines), and clathrate meltdown timescales τ_{fast} , of 1, 10, and 100 kyr (solid lines labeled with τ_{fast} value in kyr). Fast-melting fraction F values are 0.3, 0.5, and 1.0, respectively. (b) Clathrate inventory. (c) Atmospheric methane perturbation, derived from the methane release rate calculated by the model, divided by an assumed atmospheric oxidation timescale of 15 years. (d) Radiative forcing from methane and CO₂ from the $\tau_{fast} = 1$ kyr, $F = 0.3$ case (solid lines) and with no clathrates (dotted line).

(Figure 12c). This calculation neglects ocean water column oxidation of methane, and is hence a worst-case scenario. The methane perturbation is more transient than that from the CO₂, because excess methane in the atmosphere only persists during active release. Even during this time, the radiative forcing from the excess methane is smaller than that from the CO₂ perturbation (anthropogenic plus clathrate carbon) (Figure 12d). The methane radiative forcing is perhaps comparable to the radiative impact of the clathrate-derived CO₂, relative to the case of no clathrate melting. The radiative effects of the methane, and the clathrate-derived CO₂, are both greater relative to the direct anthropogenic forcing, if the anthropogenic carbon release is small. In all cases, the potential decomposition of clathrates represents a significant amplification of anthropogenic climate forcing, on timescales of 1–100 kyr.

5. Summary

[32] The kinetics of buildup and meltdown of the clathrate reservoir are shown to be central to the inventory of clathrate today, and in the past and future. The timescale of buildup controls whether the reservoir still feels the effect of climate cooling since the Miocene, and whether the clathrate reservoir loses methane during deglaciations. The timescale of meltdown, and fraction of the methane which is released relatively quickly, determine the magnitude of the melting response to anthropogenic warming. The model predicts deglacial methane releases driven by ocean warming of 200 Gton C or less, consistent with the isotopic record of δ¹³C. At the same time, the model-predicted clathrate response to anthropogenic carbon is predicted to be large; on the order of thousands of Gton C.

Acknowledgments

[33] We would like to acknowledge support from the National Science Foundation and helpful reviews by Mark Maslin and Andy Ridgwell.

References

Adkins, J. F., K. McIntyre, and D. P. Schrag (2002), The salinity, temperature, and δ¹⁸O of the glacial deep ocean, *Science*, *298*, 1769–1773.

Archer, D. E., and E. Maier-Reimer (1994), Effect of deep-sea sedimentary calcite preservation on atmospheric CO₂ concentration, *Nature*, *367*, 260–264.

Archer, D. E., A. Winguth, D. Lea, and N. Mahowald (2000), What caused the glacial/interglacial atmospheric pCO₂ cycles?, *Rev. Geophys.*, *38*, 159–189.

Archer, D. E., J. L. Morford, and S. R. Emerson (2002), A model of suboxic sedimentary diagenesis suitable for automatic tuning and gridded global domains, *Global Biogeochem. Cycles*, *16*(1), 1017, doi:10.1029/2000GB001288.

Archer, D., P. Martin, B. Buffett, V. Brovkin, S. Rahmstorf, and A. Ganopolski (2004), The importance of ocean temperature to global biogeochemistry, *Earth Planet. Sci. Lett.*, *222*, 333–348.

Berner, R. A. (1997), The rise of plants and their effect on weathering and atmospheric CO₂, *Science*, *276*, 544.

Berner, R. A., and K. Caldeira (1997), The need for mass balance and feedback in the geochemical carbon cycle, *Geology*, *25*, 955–956.

Berner, R. A., and Z. Kothavala (2001), GEOCARB III: A revised model of atmospheric CO₂ over phanerozoic time, *Am. J. Sci.*, *301*(2), 182–204.

Broecker, W. S., and T. H. Peng (1987), The role of CaCO₃ compensation in the glacial to interglacial atmospheric CO₂ change, *Global Biogeochem. Cycles*, *1*, 15–29.

Buffett, B. A. (2000), Clathrate hydrates, *Annu. Rev. Earth Planet. Sci.*, *28*, 477–507.

Buffett, B., and D. E. Archer (2004), Global inventory of methane clathrate: Sensitivity to changes in environmental conditions, *Earth Planet. Sci. Lett.*, *227*, 185–199.

Cappellen, P. V., and E. Ingall (1996), Redox stabilization of the atmosphere and oceans by phosphorus-limited marine productivity, *Science*, *271*, 493–495.

Crowley, T. J. (1995), Ice age terrestrial carbon changes revisited, *Global Biogeochem. Cycles*, *9*, 377–389.

Davie, M. K., and B. A. Buffett (2001), A numerical model for the formation of gas hydrate below the seafloor, *J. Geophys. Res.*, *106*(B1), 497–514.

Davie, M. K., and B. A. Buffett (2003), A steady state model for marine hydrate formation: Constraints on methane supply from pore water sulfate profiles, *J. Geophys. Res.*, *108*(B10), 2495, doi:10.1029/2002JB002300.

Dickens, G. R. (2001a), Modeling the global carbon cycle with a gas hydrate capacitor: Significance for the latest Paleocene thermal maximum, in *Natural Gas Hydrates: Occurrence, Distribution and Detection*, *Geophys. Monogr. Ser.*, vol. 123, pp. 19–38, AGU, Washington, D. C.

Dickens, G. R. (2001b), The potential volume of oceanic methane hydrates with variable external conditions, *Org. Geochem.*, *32*, 1179–1193.

Flemings, B. P., X. Liu, and W. J. Winters (2003), Critical pressure and multiphase flow in Blake Ridge gas hydrates, *Geology*, *31*, 1057–1060.

Gornitz, V., and I. Fung (1994), Potential distribution of methane hydrate in the world's oceans, *Global Biogeochem. Cycles*, *8*, 335–347.

Harvey, L. D. D., and Z. Huang (1995), Evaluation of the potential impact of methane clathrate destabilization on future global warming, *J. Geophys. Res.*, *100*, 2905–2926.

Hovland, M., and A. G. Judd (1988), *Seabed Pockmarks and Seepages*, Springer, New York.

Kayen, R. E., and H. J. Lee (1991), Pleistocene slope instability of gas hydrate-laden sediment of Beaufort Sea margin, *Mar. Geotech.*, *10*, 125–141.

Kvenvolden, K. A. (1988), Methane hydrate: A major reservoir of carbon in the shallow geosphere, *Chem. Geol.*, *71*(1–3), 41–51.

Kvenvolden, K. A. (1993), Gas hydrates: Geological perspective and global change, *Rev. Geophys.*, *31*(2), 173–187.



- MacDonald, G. (1990a), The future of methane as an energy resource, *Annu. Rev. Energy*, *15*, 53–83.
- MacDonald, G. (1990b), Role of methane clathrates in past and future climates, *Clim. Change*, *16*, 247–281.
- Martin, P. A., D. W. Lea, Y. Rosenthal, N. J. Shackleton, M. Sarnthein, and T. Papenfuss (2002), Quaternary deep sea temperature histories derived from benthic foraminiferal Mg/Ca, *Earth Planet. Sci. Lett.*, *198*(1–2), 193–209.
- Maslin, M. A., and E. Thomas (2003), Balancing the deglacial global carbon budget: The hydrate factor, *Quat. Sci. Rev.*, *22*, 1729–1736.
- Maslin, M. A., N. Mikkelsen, C. Vilela, and B. Haq (1998), Sea-level- and gas-hydrate- controlled catastrophic sediment failures of the Amazon Fan, *Geology*, *26*, 1107–1110.
- Maslin, M. A., M. Owen, S. Day, and D. Long (2004), Linking continental slope failure to climate change: Testing the Clathrate Gun Hypothesis, *Geology*, *32*, 53–56.
- Milkov, A. V. (2004), Global estimates of hydrate-bound gas in marine sediments: How much is really out there?, *Earth Sci. Rev.*, *66*(3–4), 183–197.
- Schrag, D. P., G. Hampt, and D. W. Murray (1996), Pore fluid constraints on the temperature and oxygen isotopic composition of the glacial ocean, *Science*, *272*, 3385–3388.
- Shackleton, N. J. (1977), Carbon 13 in *Uvigerina*: Tropical rainforest history and the equatorial Pacific carbonate dissolution cycles, in *The Fate of Fossil Fuel CO₂ in the Oceans*, edited by N. R. Andersen and A. Malahoff, pp. 401–428, Springer, New York.
- Stouffer, R. J., and S. Manabe (2003), Equilibrium response of thermohaline circulation to large changes in atmospheric CO₂ concentration, *Clim. Dyn.*, *20*, 759–773.
- Zachos, J. C., M. Pagani, L. Sloan, E. Thomas, and K. Billups (2001), Trends, rhythms, and aberrations in global climate 65 Ma to present, *Science*, *292*, 686–693.